

# Applied Mathematics and Nonlinear Sciences

<http://journals.up4sciences.org>

## Multi-scale Simulations of Dry Friction Using Network Simulation Method

F. Marín<sup>a†</sup>, F. Alhama<sup>b</sup>, J. Solano<sup>c</sup>, P.A. Meroño<sup>d</sup> and J.F. Sánchez<sup>b</sup>.

<sup>a</sup> Departamento de Ingeniería Eléctrica, Universidad Politécnica de Cartagena, 30204, Cartagena, Spain

<sup>b</sup> Departamento de Física Aplicada, Universidad Politécnica de Cartagena, 30204, Cartagena, Spain

<sup>c</sup> Institut für Fertigungstechnologie keramischer Bauteile, Universität Stuttgart, 70569, Stuttgart, Germany

<sup>d</sup> Departamento de Ingeniería Mecánica, Universidad Politécnica de Cartagena, 30204, Cartagena, Spain

### Submission Info

Communicated by Juan L.G. Guirao

Received 7th March 2016

Accepted 23th November 2016

Available online 23th November 2016

### Abstract

The study of everyday phenomena involving friction continues to maintain a high level of difficulty despite its long history. The causes of this problem lie in the different scale of the characteristics of the phenomenon, macroscopic and microscopic. Thus, very different models, valid in a narrow scope which prevents generalization, have been appearing. This survey presents the application of network simulation method to the numerical solution to the study of friction at very different scales. On the one hand, on a microscopic scale an atomic force microscope model has been studied, related to the analysis of soft surfaces at the atomic scale. Furthermore, on a macroscopic scale model related to the analysis of an industrial device, such as a brake mechanism has been studied. After presenting herein is a review of the different formulations of the friction force, the nature of the surfaces involved in the phenomenon, as well as the definition of the problems to be analyzed. The design of network models and the implementation of the initial conditions are explained. The results of the application of network models to selected problems are presented. In order to verify the reliability of the proposed models, their results are compared with the solutions obtained by other numerical methods or experimental results, one from a device developed during the preparation of this report.

**Keywords:** dry friction; stick-slip; Network Simulation Method; Atomic Force Microscope; Girling brake; Lyapunov exponents

**AMS 2010 codes:** Put here the AMS 2010 codes of the paper.

## 1 Introduction

In the text of González-Fernández [1] can be found a detailed description of the fundamentals of the method and the first applications in different fields of science and engineering: electrochemical processes, transport

<sup>†</sup>F. Marín.

Email address: [pentxo.marin@upct.es](mailto:pentxo.marin@upct.es)

through membranes, heat transfer, etc. After this date, the Network Simulation Method (NSM), has been applied to new problems developing models not covered by a specific new text, so that the person concerned should refer to the specific scientific publications or doctoral theses in the research group ‘Simulation Networks’, from University of Cartagena (UPCT), or research groups working with this method at the Universities of Granada, Jaen and Murcia: [2–7]. In this regard it should be mentioned applications in the fields of fluid flow to transport (of mass or heat), inverse problem in heat transmission, magneto-hydrodynamic flow, mechanical vibrations, tribology, dry friction, membrane transport, elasticity, development of specific numerical calculation programs, etc. NSM had already been successfully applied in various fields of engineering, such as heat transfer [7, 11], electrochemical reactions [12, 13], transport across membranes [14], inverse problems [15–18], ion transport, magneto-hydrodynamics [19], problems coupled flow and transport [17, 20–22]; Alhama, Soto and al 2012), and others [23–26]; all these works describe nonlinear transport processes. In addition, recently, it has been applied to mechanics of deformable solids [27], and dry friction at the atomic level.

On the other hand, there have been various programs that use the NSM as a tool for numerical calculation: PRODASIM for designing simple fins [28], PROCCA\_09 for design and optimization of thermal problems [29], FATSIM\_A for simulating flow fluids with solute transport problems [30], FAHET for simulation of flow fluids with heat transfer problems [31], EPSNET\_10 for simulation problems elasticity [32] and OXIPSIS\_12 for simulating corrosion problems [33].

The formal equivalence between the network model and the physical process is that both are governed by the same differential equations in finite difference in space, covering both the elementary cell volume or as to the boundary conditions. However, time remains continuous variable in the design model.

The formal approach, which is the basis for the development of the problems, is the ‘Network Theory’ of Peusner [34], in which his ‘thermodynamics of networks’ is supported; this theory, in turn, is based on the theory of circuits from a generalization of their conjugate variables, electric current and potential difference. Network models are for Peusner an accurate representation of the mathematic characteristic of the processes described. Thus, the variable velocity and displacement, characteristics of the problems, must satisfy Kirchhoff’s laws and their relationships determine the corresponding circuit elements. However, in each individual process and once conjugate variables chosen, the information on which circuit elements involved in the network model and how they connect with each and other, is obtained from the mathematical model and not on considerations of physical type on the role playing these variables.

In summary, in network theory, the feasibility of a network model involves:

- The existence of an independent network of time
- The existence of a conserved quantity called flow associated with each branch, connecting nodes and obeys the laws of Kirchhoff currents (LCK)
- The existence of a magnitude that satisfies criteria of uniqueness associated with each node, and obeys the Kirchhoff voltage law (KVL)

It is going to be showed different models of application of the method to different fields of engineering to be presented in the second section. In the third, the governing equations, and its transposition into network models in the fourth. Applications are going to be shown in the fifth section, concluding with the conclusions in the sixth.

## 2 MULTI-SCALE PROBLEMS

To show the most practical aspects of the method, applications at different scales of the same physical problem, dry friction, will be described. This allows us to probe the flexibility of the method to exploit those

portions of code developed for a given application to another which has quite different elements. This capability allows efficiently address problems that occur at very different scales. From this perspective, it is interesting to work with elements, circuit components, which can represent very different scales phenomena.

From this perspective there are several problems that must be addressed from very different scales, so even coupled, such as stress analysis in ceramic coatings of metal parts. In this type of problems the most important difficulty is to exchange information between macro and micro scales.

However, in this work, in order not to overcomplicate the exhibition uncoupled problems have been chosen. Specifically, there has been the analysis of two devices: atomic force microscopes, dry friction at the atomic scale, and Girling brakes, dry friction in a device of industrial application. The first problem is formulated considering physical associated with crystalline structures under study of the mentioned microscope, while the second is the object of mechanics more applied.

### 3 ATOMIC SCALE PROBLEM

Atomic scale dry friction phenomenon is analyzed through Network Simulation Method implemented models, specifically 'dry friction between microscope tip and smooth surface at atomic-scale'.

This study will analyze the phenomenon of dry friction at the atomic scale using models implemented by the network simulation method, namely the microscope frictional force (FFM), evolution of the microscope scanning force (SFM), increases research capacity of phenomena at the atomic scale, key issue for understanding the origin and nature of the fundamental laws of friction. The analysis of the behavior of these point contacts is done by a two-dimensional model of friction at the atomic scale. The response of the tip is the 'stick-slip' type [35].

After a detailed review of the literature a number of techniques and materials for analysis have been selected. The cases are:

- NaF (001): it is a surface with translational symmetry. In this case the FFM is used [36]
- Highly Oriented Pyrolytic Graphite (HOPG) is well-defined structures sheets, often chemically stable. In this case an SFM and LFM are used [37]
- Graphite: the AFM is used [38]

#### 3.1 The Governing Equations

The AFM, SFM, FFM tip physical scheme on a sample surface model, Fig. 1, assumes one rigid sliding body connected by three springs (one for each spatial direction) to the mobile microscope support. Each spring reflects the elastic interaction between the two surfaces during the contact [36, 38]. The sliding body involves inertial effect and the interaction with the sample surface.

The hypotheses currently assumed in FFM, AFM and SFM models are: (i) the microscope support is rigid and moves at a constant velocity,  $v_M$ , (ii) the cantilever and the tip show elastic behaviour, and (iii) interactional force between the tip and the sample surface is a function of the relative distances between the tip and the atoms forming the sample surface.

Several forces act on the tip in x-direction: inertial force represented by  $m \cdot (d^2x_t/dt^2)$ , where  $x_t$  is the absolute displacement of the tip of mass  $m$ ; elastic force from the spring, represented by the term  $k_x \cdot (x_M - x_t)$ ; and damping force represented by the term  $c_x \cdot (dx_t/dt)$ . The coefficients of these forces are constants. Similar forces act in the other directions. In addition, the interaction force between the tip and the sample surface is implemented from a surface potential [36, 38]. Thus, the surface potential for NaF with an FFM tip, as used by

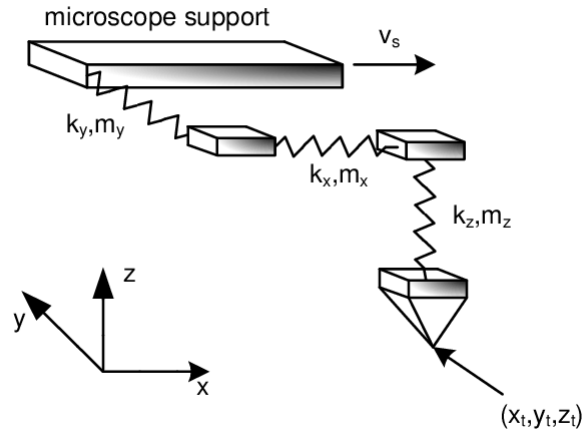


Figure 1 Model of AFM, FFM and AFM tip

Hölscher et al. [36] is:

$$V(x_t, y_t) = -V_0 \cdot \cos\left(\frac{2\pi}{a_x} \cdot x_t\right) \cdot \cos\left(\frac{2\pi}{a_y} \cdot y_t\right) \quad (1)$$

where the potential amplitude,  $V_0$ , is  $1\text{eV}$ , while  $a_x$  and  $a_y$ , the double of the lattice constant, are  $4.62$  for both parameters. Hölscher et al. [37] use a slight modification of Eq. 1 to study HOPG with a SFM tip:

$$V_{HOPG}(x_t, y_t) = -V_0 \cdot \left[ 2 \cdot \cos\left(\frac{2\pi}{a} \cdot x_t\right) \cdot \cos\left(\frac{2\pi}{a\sqrt{3}} \cdot y_t\right) + \cos\left(\frac{4\pi}{a\sqrt{3}} \cdot y_t\right) \right] \quad (2)$$

where  $V_0$  is  $0.5\text{eV}$  and the lattice constant,  $a$ , is  $2.46\text{\AA}$ . Sasaki et al. [38] used the Lennard-Jones potential to study the graphite with an AFM tip:

$$V_{TS} = \sum_i 4\epsilon \cdot \left[ \left(\frac{\sigma}{r_{0i}}\right)^{12} - \left(\frac{\sigma}{r_{0i}}\right)^6 \right] \quad (3)$$

where the strength of the potential,  $\epsilon$ , is  $0.87381 \cdot 10^{-2}\text{eV}$ , and the value of the distance between the tip and the surface atom at which the potential is zero,  $\sigma$ , is  $2.4945\text{\AA}$ . The distance between the tip and the  $i$ -th atom of the surface,  $r_{0i}$ , is calculated from the  $i$ -th atom position inside the lattice, which is defined by its constant,  $2.46\text{\AA}$ , and the nearest distance between 2 carbon atoms,  $1.424\text{\AA}$ . Hölscher et al. used the same potential with the same sample surface and microscope [39], but  $\sigma$  is equal to  $3.4\text{\AA}$ .

As a result of the balance of the forces on the tip, Fig. 1, the following equations can be written:

$$\begin{cases} m \cdot \ddot{x}_t = k_x \cdot (x_M - x_t) - \frac{\partial V}{\partial x_t} - c_x \cdot \dot{x}_t \\ m \cdot \ddot{y}_t = k_y \cdot (y_M - y_t) - \frac{\partial V}{\partial y_t} - c_y \cdot \dot{y}_t \\ m \cdot \ddot{z}_t = k_z \cdot (z_M - z_t) - \frac{\partial V}{\partial z_t} - c_z \cdot \dot{z}_t \end{cases} \quad (4)$$

where  $x_M$ ,  $y_M$  and  $z_M$  are the microscope support displacements over the three coordinates.

The movement of the microscope support is a set of trips in the  $x$ -direction. For each of these trips, the initial condition of tip displacement in the  $x$ -direction is null, and in the  $z$ -direction is null except for the AFM tip on

graphite sample. In the y-direction, the initial condition for this displacement is the same as for the microscope support. The initial condition of tip velocity is null for each direction.

#### 4 MACROSCOPIC SCALE PROBLEM

The physical phenomenon of dry friction between sliding bodies is an important subject in mechanical engineering and many studies have been devoted to it [40–44]. An example of dry friction is found in the Antilock Braking System (ABS), which prevents the wheels from locking up and stops a vehicle at a much faster rate and with better control than a driver could manage. The simplest antilock braking device is represented by a nonlinear bi-dimensional dynamic system.

A source of the nonlinearity of this system is the relationship between the sliding process and the dynamic friction coefficient. Most classical friction models map the friction coefficient against the relative velocity in a static way. The shape of such characteristics is the same for qualitatively different dynamic responses (periodic, quasi-periodic, chaotic or stochastic), which means that the friction force is independent of the character of the motion, i.e., insensitive to the system dynamics (insensitive friction models). The term frictional memory [45] has been coined to refer to a pure delay between relative velocity and friction force [45] without reference to any specific model. Thus, hysteretic effects of frictional memory, such as frictional lag [46], pre-sliding displacement [47, 48], non-reversibility [49], break-away force [50, 51] and Stribeck effect [52], could explain it. The inclusion of these effects in friction models causes the friction characteristics to become motion-sensitive (sensitive friction models). It should be pointed out that the strong nonlinearity of the relative velocity near zero is the main problem when modelling the numerical switching algorithms [53]. Two examples of insensitive friction models are the classical Coulomb model [54], with a constant value of the kinetic friction coefficient, and the well-known Popp-Stelter approach with a nonlinear kinetic friction and Stribeck effect [14]. A model with symmetrical non-reversible characteristic and an exponential function of the relative acceleration is an example of the sensitive friction model [55].

Awrejcewicz used a physical model of a braking system for each wheel, which involves nonlinear coefficients [56–61]. To be more precise, a Girling ‘duo-servo’ brake [62], Fig. 2. To simplify the study of the system, it is usual to consider a sliding block, which represents the brake pad, and a rotational crank, Fig. 3, [56, 63–65]. The sliding block is jointed to the chassis by a linear spring, with a stiffness  $k_1$ , and to the crank by two springs, with stiffness  $k_2$  and  $k_3$  for the horizontal and vertical directions, respectively. The elastic interaction between the brake pad and the drum brake is neglected. The belt velocity is represented by  $v_{dr}$ .

The solution of the dynamic problems is very sensitive to the range of the parameters involved in the problem: (i) parameters in dynamic friction coefficient, (ii) translational stiffness between the sliding surfaces and (iii) constant velocity.

The scheme used to analyse this mechanical system is the same employed in other friction problems studied by the authors [66, 67], and is at the core of a software application under development. For this reason, an exhaustive review of the state of the art is necessary, systematizing the different formulation of friction processes: Atomic Friction Microscope models [66] and macroscopic models [67].

The aim of this work is to use the rules of network simulation [1] to design a reliable and efficient network model for the stick-slip phenomenon, that can be simulated in commercial software of circuit analysis such as PSpice [68, 69]. The model, which provides both transient and steady state solutions, is based on the formal equivalence between the finite-difference equations of the mathematical and network models, an equivalence that goes beyond the scope of classical electrical analogy of many books [70, 71], which mainly deal with linear problems. The network method is a numerical tool whose efficiency has been demonstrated in many science and engineering problems, including heat transfer, electrochemistry, fluid flow and solute transport, inverse problems, etc. [72–75]. Once the equivalence between electric and mechanical variables has been chosen, linear

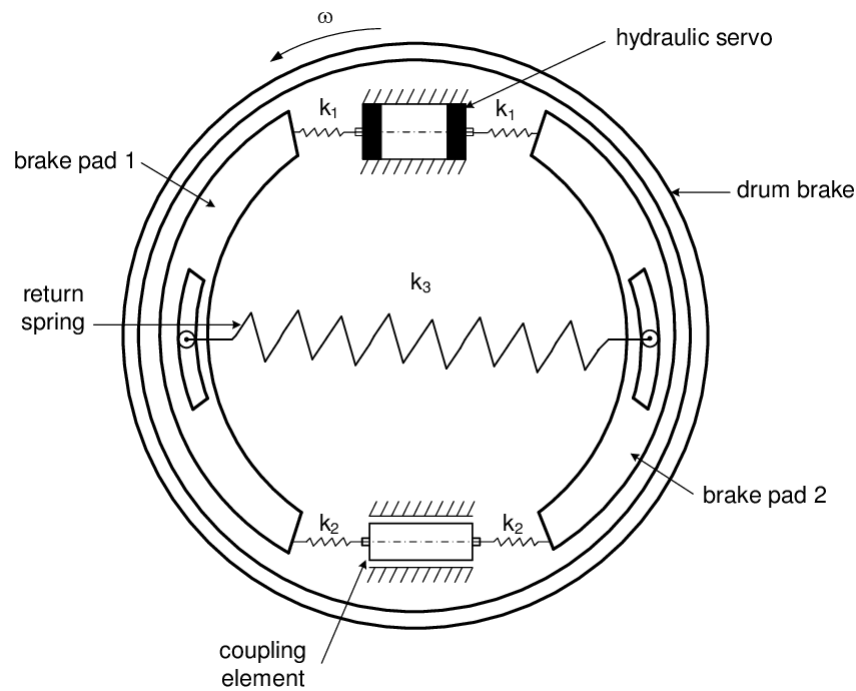


Figure 2 Drawing of a 'duo-servo' Girling brake

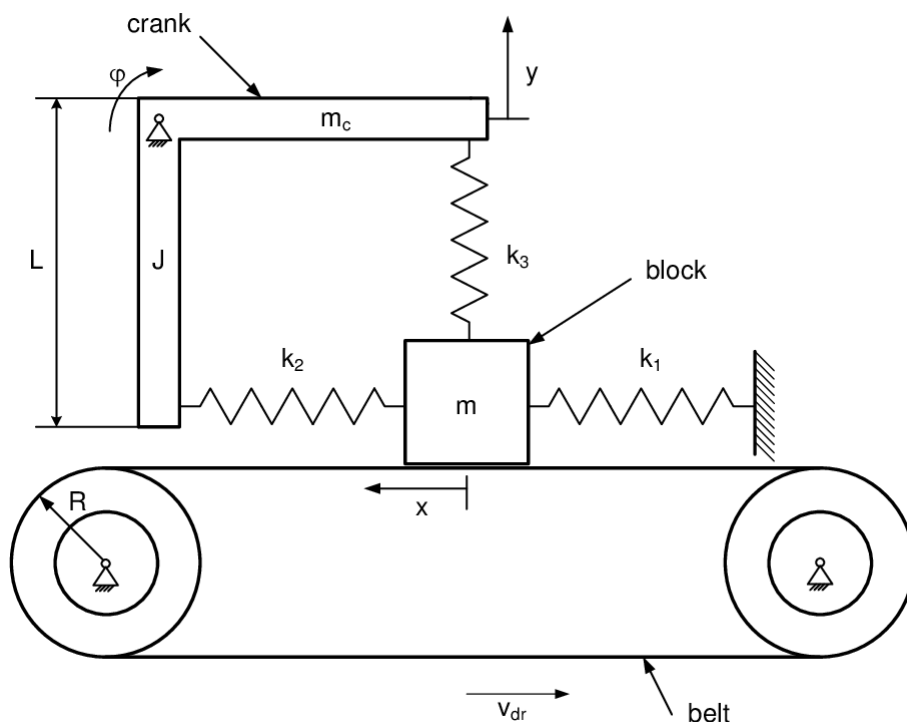


Figure 3 The scheme of the mechanism represented in Fig. 2

terms of the PDE are easily implemented by linear electrical devices, such as resistors, capacitors and coils, while non-linear and coupled terms are implemented using auxiliary circuits or controlled current and voltage sources. The last are a special kind of source whose output can be defined by software as a function of the de-

pendent or independent variables determined in any node or any electrical component of the model. In addition, boundary and initial conditions - whether linear or not - are also immediately implemented by suitable electric components. Once the network model has been designed, it is run with no need for other mathematical manipulations since the simulation code does this. The well-trying and powerful software for circuit simulation, PSpice, requires relatively short computing times thanks to the continuous adjustment of the internal time step required for the convergence. In addition, the solution simultaneously provides all the variables of interest: displacements and velocities.

#### 4.1 The Governing Equations

Several forces act on the block: inertial force, represented by  $m \cdot \frac{d^2x}{dt^2}$ , where  $x$  is the absolute horizontal displacement of the block of mass  $m$ , and the elastic forces from the two springs, represented by the terms  $-k_1 \cdot x$  and  $-k_2 \cdot (x - y)$ . Similar forces act on the crank: inertial force, represented by  $J \cdot \frac{d^2y}{dt^2} / L$ , where  $y$  is the absolute vertical displacement of the horizontal arm tip of the crank with inertial moment of  $J$ , and the elastic forces from the two springs, represented by the terms  $-k_3 \cdot y \cdot L$  and  $-k_2 \cdot (y - x) \cdot L$ . The coefficients of these forces are constant. In addition, the interaction force between the block and the belt is implemented by [76, 77].

$$\begin{cases} |F_f| \leq \mu_s \cdot F_N = F_s; \text{ if } v_{rel} = 0 \\ F_f = -\text{sgn}(v_{rel}) \cdot \mu \cdot F_N; \text{ if } v_{rel} \neq 0 \end{cases} \quad (5)$$

In Eq. 5, the first equation represents the stick phase, when the block has the same velocity that the belt. In this case, it is not necessary to solve the dynamic equation to get information about the block velocity. The second equation represents the slip phase, with the block slipping, and the dynamic equation is used in order to obtain the acceleration. The friction force is governed by Coulomb's Law, which involves step function.

From Eq. 5, it is possible to distinguish two physical phases: stick and slip. Stick is controlled by the following single equation

$$\dot{x} = v_{dr} \quad (6)$$

whereas slip phase is controlled by a more complex equation. Thus, as a result of the balance of the forces on the block and on the crank, the following equations can be written

$$\begin{cases} m \cdot \ddot{x} + k_1 \cdot x + k_2 \cdot (x - y) = F_k(v_{rel}) \\ J \cdot \frac{\ddot{y}}{L} + k_3 \cdot y \cdot L - k_2 \cdot (x - y) \cdot L = 0 \end{cases} \quad (7)$$

where  $F_k$  is a more complex version of  $F_f$ , which involves the relative velocity effect.

As other authors, we also consider  $k_2 = k_1$  [56, 63–65]

The parametrized Eq. 7 is given by

$$\begin{cases} \frac{m}{k_1} \cdot \frac{d^2x}{dt^2} + 2x - y = -\mu \cdot \left( -\frac{k_3}{k_1} \cdot y + \frac{m}{k_1} \cdot g + \frac{m_c}{k_1} \cdot g \right) \cdot \frac{2}{\pi} \cdot \frac{\arctan(\varepsilon \cdot v_{rel})}{1 + \delta \cdot |v_{rel}|} \\ \frac{J}{k_1 \cdot L^2} \cdot \frac{d^2y}{dt^2} - x + \frac{k_1 + k_3}{k_1} \cdot y = 0 \end{cases} \quad (8)$$

In the Eq. 8,  $\varepsilon \cdot v_{rel}$  is a nondimensional magnitude, and so  $\varepsilon$  has the dimension s/m. The last term of the first equation of Eq. 8 represents  $F_k/k_1$ . The friction force magnitude is calculated from the normal reaction, an addition of weights and a spring force. The sign function is assessed by arctangent.



To simplify Eq. 8, it is necessary to define a nondimensional time,  $\tau = \sqrt{k_1/m}$ . Thus, the Eq. 8 can be written as

$$\begin{cases} \frac{d^2x}{d\tau^2} + 2x - y = -\mu \cdot \left( -\frac{k_3}{k_1} \cdot y + g' \right) \cdot \frac{2}{\pi} \cdot \frac{\arctan(\varepsilon' \cdot v'_{rel})}{1 + \delta' \cdot |v'_{rel}|} \\ \frac{J}{m \cdot L^2} \cdot \frac{d^2y}{d\tau^2} - x + \frac{k_1 + k_3}{k_1} \cdot y = 0 \end{cases} \quad (9)$$

where  $J/m \cdot L^2$  is the parameter  $\xi$ , and  $k_1 + k_3/k_1$  is the nondimensional parameter  $\kappa$ . Eq. 9 can be written as

$$\begin{cases} \frac{d^2x}{d\tau^2} + 2x - y = -\mu \cdot ((1 - \kappa) \cdot y + g') \cdot \frac{2}{\pi} \cdot \frac{\arctan(\varepsilon' \cdot v'_{rel})}{1 + \delta' \cdot |v'_{rel}|} \\ \xi \cdot \frac{d^2y}{d\tau^2} - x + \kappa \cdot y = 0 \end{cases} \quad (10)$$

The initial horizontal displacement of the block is null, as is the vertical displacement of the horizontal arm tip of the crank. The initial velocity of the block is the belt velocity and the vertical velocity of the horizontal arm tip of the crank is null.

## 5 NETWORK MODELS

The solution of the problems mentioned above involves solving the equations developed further considering the boundary and initial conditions for each case. In the following paragraphs the network model corresponding to the governing equation for each of the problems mentioned is deduced.

### 5.1 Atomic Force Microscope

The initial conditions related to displacements,  $x_M - x_t = y_M - y_t = z_M - z_t = 0$ , and velocities,  $dx_t/dt = dy_t/dt = dz_t/dt = 0$ , are introduced in the specifications of the initial conditions of the capacitors (initial voltage value) and of the coils (initial current value), respectively. The whole network model is now run in a Duo Core, using the code PSpice [68,69] and very few rules are required since the model contains very few electrical devices.

The design of a reliable network model requires a formal equivalence between the equations of the model and those of the process, including the initial conditions. Since Eq. 4, the basic network model is related to this equation, to which initial conditions must be added. Basic rules for designing the model can be found in González-Fernández [1]. The first step is to choose the equivalence between mechanical and electric variables (different choices give rise to different networks). For the problem under consideration, the following equivalence is established:  $x_t$  (tip displacement in the x-direction)  $\equiv q$  (electric charge in the network), or  $dx_t/dt$  (tip velocity in the x-direction)  $\equiv dq/dt = i$  (electric current at the network). In the other directions, similar equivalences are applied.

Now, each term of the Eq. 4 is considered as a voltage in an electric component whose constitutive equation is defined by the mathematical expression of such a term. Hence, the equation itself can be considered as a voltage balance (second Kirchhoff's law) of a network that contains as many electrical components connected in series as there are terms in the equation. The linear term of Eq. 4,  $d^2x_t/dt^2$ , is associated to a coil (inductance) since the constitutive equation of this component is  $V_L = L(di/dt) = L(d^2q/dt^2)$ , with  $L = 1H$ . The same electrical element is used for the other two directions. The non-linear terms cannot be implemented directly, and require the use of controlled current (or voltage) sources or auxiliary circuits. The first are devices whose output is de-



finied by software as an arbitrary, continuous mathematical function of the dependent variables: voltages at any node of the network or the current in any component. This capability, which is beyond the scope of the classical electrical analogy that appears in most text books, makes the network method an interesting and efficient tool in the field of numerical computation.

To implement the term  $x_t$ , the value of this variable must be determined by integrating the current in the network model,  $dx_t/dt$ . To this end, an auxiliary circuit is implemented, Fig. 4(b), in the models of FFM on the NaF sample; Fig. 5(c) in the model of AFM on a graphite sample. The terms  $y_t$  and  $z_t$  are implemented in similar network models.  $F_{1x}$  is the controlled current source whose output is the current,  $dx_t/dt$ , that crosses the voltage generator (used as an ammeter),  $V_x$ . The voltage of this generator is zero so as not to disturb the network model of 4. The current of  $F_{1x}$  is integrated using a capacitor with  $C_{x1} = C_{y1} = C_x = 1F$ ; in this way, the voltage through this capacitor,  $V_{Cx1} = V_{Cy1} = V_{Cx} = C_{x-1} \int (dx_t/dt)dt$ , is simply the variable  $x_t$  (a resistor of very high value,  $R_{INF}$ , is needed for electrical continuity).

Once the variable  $x_t$  has been determined, a controlled voltage source is used to implement the term  $k_x \cdot (x_M - x_t)$  in the model  $E_2$  in the models of FFM on NaF sample. For the models of AFM on graphite, the controlled voltage source is  $E_{Tx1}$ . The variable  $x_M$  is obtained as the product of the microscope support velocity and time, and is provided by the auxiliary circuit shown in Fig.4(c). The term related to  $\frac{\partial V}{\partial x_t}$  is implemented by a pair of controlled voltage sources,  $E_1$  and  $E_{1a}$ , for FFM on the NaF sample. For the models of AFM on graphite sample, the controlled voltage source is  $E_{Tx2}$ . When the potential used is a Lennard-Jones potential, an auxiliary circuit is implemented, Fig. 5(b), for the model of AFM on graphite sample. The terms related to  $\frac{\partial V}{\partial y_t}$  and  $\frac{\partial V}{\partial z_t}$  are implemented in a similar way. The last term of the first equation in Eq. 4 is implemented by a resistor with a resistance of  $c_x$  in the models of FFM on NaF sample. The last term of the other equations in Eq. 4 is implemented in similar form. The initial conditions related to displacements,  $x_M - x_t = y_M - y_t = z_M - z_t = 0$ , and velocities,  $dx_t/dt = dy_t/dt = dz_t/dt = 0$ , are introduced in the specifications of the initial conditions of the capacitors (initial voltage value) and of the coils (initial current value), respectively. The whole network model is now run in a Duo Core, using the code PSpice [68, 69] and very few rules are required since the model contains very few electrical devices.

## 5.2 Girling Brake

The design of a reliable network model requires the formal equivalence between the equations of the model and those of the process, including the initial conditions. The basic network model is related to Eq. 10 to which initial conditions must be added. Basic rules for designing the model can be found in González-Fernández [1]. The first step is to choose the equivalence between mechanical and electrical variables (different choices give rise to different networks). For the problem under consideration, the following equivalences are established:  $x$  (horizontal displacement of the block)  $\equiv q_1$  (electric charge in the network),  $y$  (vertical displacement of the horizontal arm tip of the crank)  $\equiv q_2$  (electric charge in the network), or  $dx/d\tau$  (velocity of the block)  $\equiv dq_1/dt = i_1$  (electric current at the network),  $dy/d\tau$  (vertical velocity of the horizontal arm tip of the crank)  $\equiv dq_2/dt = i_2$  (electric current at the network).

Now, each term of Eq. 10 is considered as a voltage in an electric component whose constitutive equation is defined by the mathematical expression of such a term. Hence, the equation itself can be considered as a voltage balance (Kirchhoff's second law) of a network that contains as many electrical components connected in series as there are terms in the equation. The linear terms of Eq. 10,  $d^2x/d\tau^2$  and  $d^2y/d\tau^2$ , are associated to two coils (inductances) since the constitutive equation of this component is  $V_L = L(di/dt) = L(d^2q/dt^2)$ , with  $L = 1H$ . Thus, the coils used in the network model have inductances of  $L_1 = 1H$  and  $L_{1A} = \xi = J/mL^2$ . The non-linear terms cannot be implemented directly, and require the use of either controlled current (or voltage) sources or auxiliary circuits. The first are devices whose output is defined by software as an arbitrary, continuous mathe-

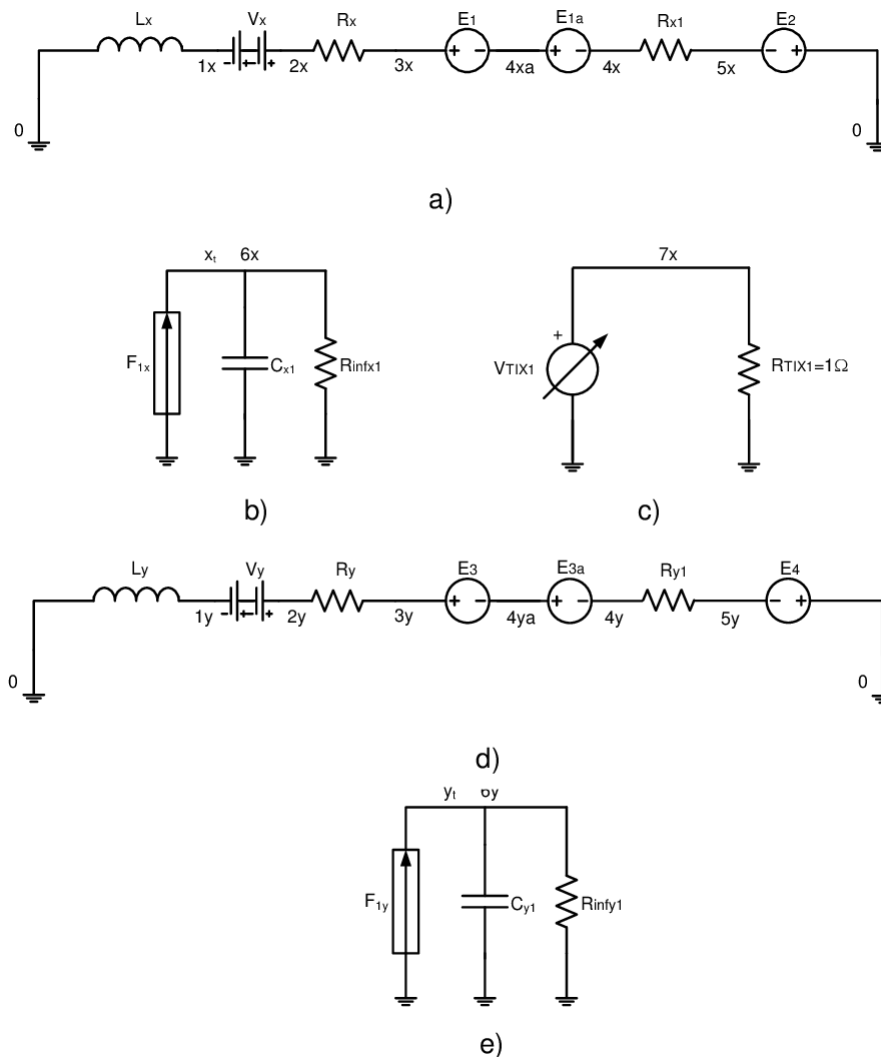


Figure 4 Network model, in  $x$  and  $y$  directions, of FFM on NaF and SFM on HOPG. a) and d) Main circuits, b) and e) auxiliary circuits to obtain  $x_t$  and  $y_t$ , and c) auxiliary circuit to obtain the time.

mathematical function of the dependent variables: voltages at any node of the network or currents in any component. This capability, which is beyond the scope of the classical electrical analogy that appears in most text books, makes the network method an interesting and efficient tool in the field of numerical computation.

To implement the terms  $x$  and  $y$ , the values of these variables must be determined by integrating the currents,  $dx/d\tau$  and  $dy/d\tau$ , in the network model. To this aim, two auxiliary circuits are implemented, Fig. 6(b) and Fig. 6(h).  $F_1$  and  $F_{1A}$  are controlled current sources whose outputs are the currents,  $dx/d\tau$  and  $dy/d\tau$ , which cross the voltage generators (used as ammeters),  $V_1$  and  $V_{1A}$  respectively. The voltage of these generators is zero so as not to disturb the network model of Eq. 10. The current of  $F_1$  is integrated using a capacitor with  $C_1 = 1F$ ; in this way, the voltage through this capacitor,  $V_{C1} = C_1^{-1} \int (dx/d\tau) d\tau$ , is simply the variable  $x$  (a resistor of very high value,  $R_{INF1}$ , is needed as a requirement of electrical continuity). In the same way, the current of  $F_{1A}$  is integrated using a capacitor with  $C_{1A} = 1F$ , the voltage through which is the variable  $y$  (another resistor of very high value,  $R_{INF1A}$ , is needed as a requirement of electrical continuity).

Once these variables have been determined, a controlled voltage source is used to implement the term  $2 \cdot x - y$  for the model; this is  $E_1$ . In the same way, a controlled voltage source is used to implement the term  $-x + \kappa \cdot y$

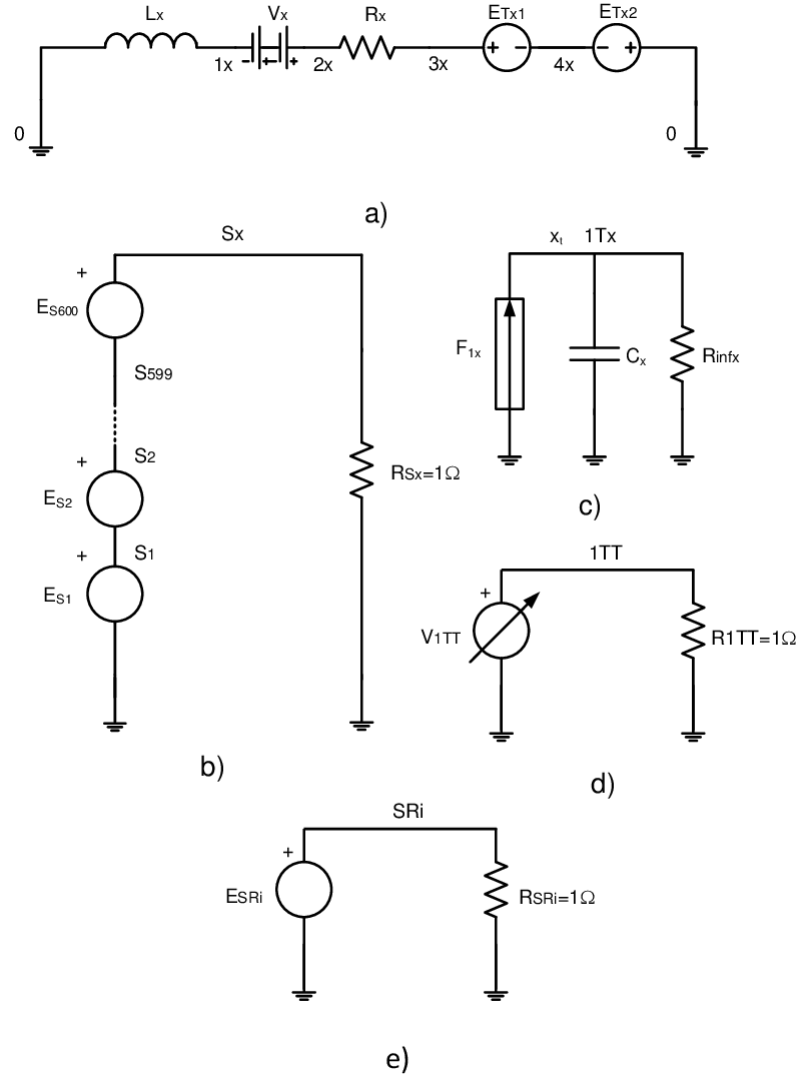


Figure 5 Network model, in x direction, of AFM on graphite. a) Main circuit, b) auxiliary circuit to obtain the force from Lennard-Jones potential, c) auxiliary circuit to obtain  $x_t$ , d) auxiliary circuit to obtain the time, and e) auxiliary circuit to obtain the square of the distance between the AFM tip and the carbon atom.

for the model; this is  $E_{1A}$ . The last term of the first equation in the system described in Eq. 10,  $\mu \cdot ((1 - \kappa) \cdot y + g') \cdot 2/\pi \cdot \arctan(\epsilon' \cdot v'_{rel}) / (1 + \delta' \cdot |v'_{rel}|)$ , is also implemented by a controlled voltage source,  $E_2$ , and requires the variable  $dx/d\tau$ . This is a problem because this variable is also the current that crosses this controlled voltage source. To solve this problem an auxiliary circuit represented in Fig. 6(f) provides the voltage used in  $E_2$ . To help this auxiliary circuit, another one is needed, Fig. 6(e), which calculates  $2/\pi \cdot \arctan(\epsilon' \cdot v'_{rel}) / (1 + \delta' \cdot |v'_{rel}|)$ .

The conditions that select the stick or the slip phase are implemented by two voltage controlled switches,  $S_1$  and  $S_2$ , following the flowchart represented in Fig. 10. To implement this, it is necessary to obtain the voltages that appear in it by using the auxiliary circuits represented in Figs. 6(c), 6(d) and 6(e). The voltage provided by controlled voltage source  $E_{control}$ , in Fig. 6(c), is a scalar associated to the slip phase when the voltage of  $E_{Elas}$ , in Fig. 3(d), is bigger than the voltage of  $E_{FRS}$ , Fig. 6(e). Otherwise, there are two possibilities: if the current that crosses  $L_1$  is not equal to the belt velocity, then the voltage of  $E_{control}$  will provide the same value

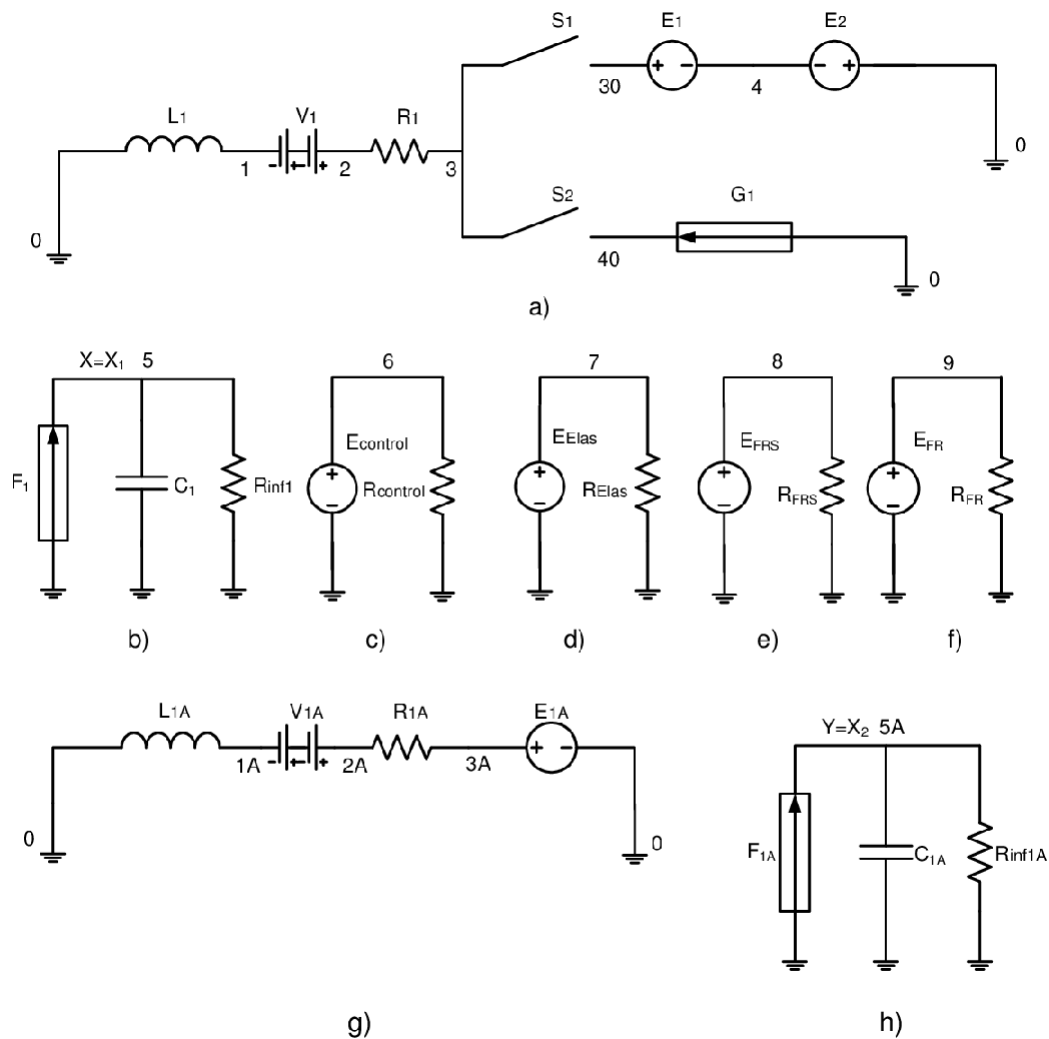


Figure 6 Network model. a) and g) Main circuits, b) and h) auxiliary circuits to get  $x$  and  $y$ , c) auxiliary circuit which control switches, d) auxiliary circuit which controls the transition between stick and slip phases, and e) and f) auxiliary circuits to obtain  $E_2$

of this scalar of the last case; if not, another check will be necessary. When the voltage in the coil is not equal to zero, then this controlled voltage source provides the same value of this scalar, which is the slip phase. If this is not the case, stick phase arises. The voltage of controlled voltage source  $E_{Elas}$ , in Fig. 6(d), provides the absolute value of the force in the horizontal springs, while controlled voltage source  $E_{FRS}$ , in Fig. 6(e), provides the maximum friction force.

Thus, if  $S_1$  is closed (stick phase), then the current will be determined by the Eq. 6. On the other hand, if  $S_1$  is open  $S_2$  will be rapidly closed (slip phase) and the current will be determined by the Eq. 7.

The initial conditions of the problem are implemented by the initial conditions of the capacitors and coils. The full network model is run on a Core Duo processor, using PSpice code [69, 78, 79].

## 6 SIMULATION RESULTS

### 6.1 Atomic scale friction simulation: atomic force microscope

The Network Simulation Method has been applied to sample surfaces and tips for which data are available: FFM tip on NaF [36], SFM tip on HOPG [37], and AFM tip on graphite [39]. The first sample has a cubic crystal net and the others have a hexagonal crystal net, which tests the potential of the network model. The characteristics of the tip, the test conditions and the sample size for the different tests are:

- the FFM tip on NaF sample is characterized by  $m_x = m_y = 10^{-8} \text{ kg}$ ,  $c_x = c_y = 10^{-3} \text{ N} \cdot \text{s/m}$  and  $k_x = k_y = 10 \text{ N/m}$ . The microscope support moves with a constant velocity of  $400 \text{ Å/s}$ , and the results are depicted with a scan range of  $20 \times 20 \text{ Å}$  and scan angle of  $0$  [36]. The proposed model solves the Eq. 4 using the potential defined in Eq. 1.
- the SFM tip on HOPG sample is characterized by  $m_x = m_y = 10^{-8} \text{ kg}$ ,  $c_x = c_y = 10^{-3} \text{ N} \cdot \text{s/m}$  and  $k_x = k_y = 25 \text{ N/m}$ . The microscope support moves with constant velocity of  $400 \text{ Å/s}$ , and the results are depicted with a scan range of  $20 \times 20 \text{ Å}$  and scan angle of  $7$ . The surface of the sample is composed of 271 hexagons with a carbon atom in each vertex (600 altogether); and it is assumed that the sample surface has a very high stiffness [37].
- the AFM tip on graphite is characterized by  $c_x = c_y = 0 \text{ N} \cdot \text{s/m}$ ,  $k_x = k_y = 0.25 - 2.5 \text{ N/m}$ ,  $k_z = 0.25 \text{ N/m}$ , and a vertical displacement of  $-6 \text{ Å}$  for the tip. The results are depicted with a scan range of  $9.8 \times 8.5 \text{ Å}$  and scan angle of  $15$  [38]. Besides,  $m_x = m_y = 10^{-6} \text{ kg}$  and a constant velocity of  $10 \text{ Å/s}$  for the microscope support, parameters not mentioned by Sasaki et al. [38], were assumed to obtain results similar to theirs.

Eq. 4 is solved in each test for the potential functions defined in the following equations:

- Eq. 1 in the FFM tip on NaF sample model
- Eq. 2 in the SFM tip on HOPG sample model
- Eq. 3 in the AFM tip on graphite sample model

In the last case, for graphite sample, only short computational times are necessary for the software to find the right values of the parameters not supplied by Sasaki et al. [38]. Fig. 7(b) shows the components of the tip elastic force,  $F_x$  and  $F_y$ , in each position on the NaF sample surface, whose crystal net is shown in Fig. 7(a). The correspondence between both depicted images enables us to use this software as a tool to interpret those images from the microscope. Thus, this software is able to manage different theoretical crystal nets, even with crystallographic defects, providing the corresponding theoretical elastic forces, which can be compared with those from the microscope. The results of the simulation agree with those obtained by Hölscher et al. [36].

Fig. 8(b) shows the components of the tip elastic force,  $F_x$  and  $F_y$ , in each position on the HOPG sample surface, whose crystal net is shown in Fig. 8(a). The results of the simulation agree with those obtained by Hölscher et al. [37]. Besides, Fig. 9(b) shows the x-direction component of the tip elastic force,  $F_x$ , in each position on the graphite sample surface, whose crystal net is shown in Fig. 9(a). In this case, a 3D graph is used to show the details better, to be more precise the stick - slip mechanism. The lines of the graph are traced at different y-coordinates, separated by a fixed step. When one of these lines crosses the sample surface at a critical position, the instabilities appear, Fig. 9(b). These critical positions have a relation with the minimal threshold of the distance between the tip and the atom on the surface. The results of the simulation agree with those obtained by Sasaki et al. [38].

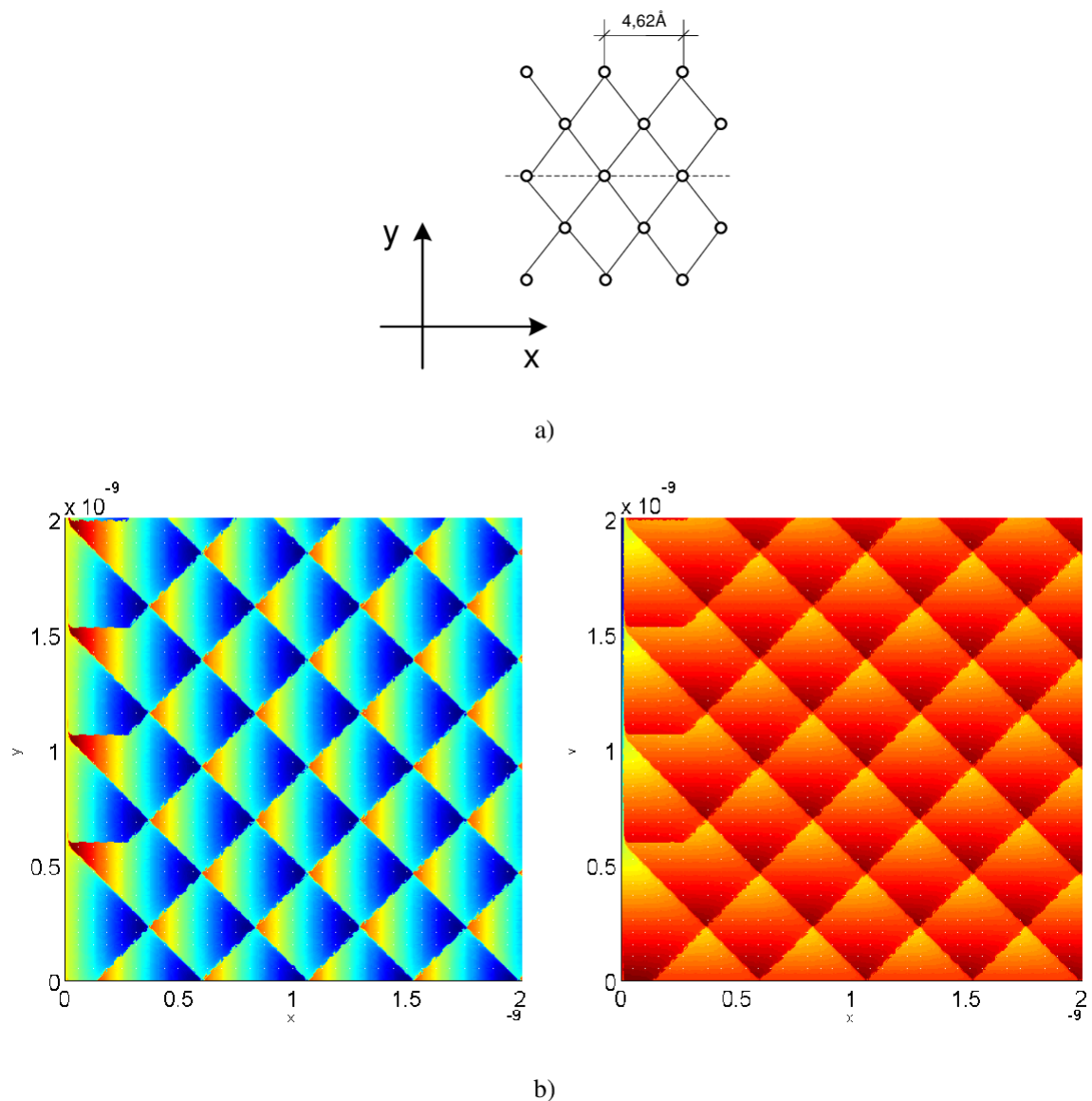


Figure 7 a) Position of the atoms in the NaF crystal net; b) Elastic force in the tip:  $F_x$  in the left hand side and  $F_y$  in the right hand side.

## 6.2 Macroscopic scale friction: Girling brake

The model used in this numerical simulation follows the mechanism shown in Fig. 11, and is similar to that used by Awrejcewicz et al [56]. Its dimensions and properties are:

- crank arm length,  $L = 0.105m$
- drum radius,  $R = 0.11m$
- crank mass,  $m_c = 0.215kg$
- block mass,  $m = 0.174kg$
- spring stiffness,  $k_1 = k_2 = 214.62N/m$ , and  $k_3 = 107.31N/m$

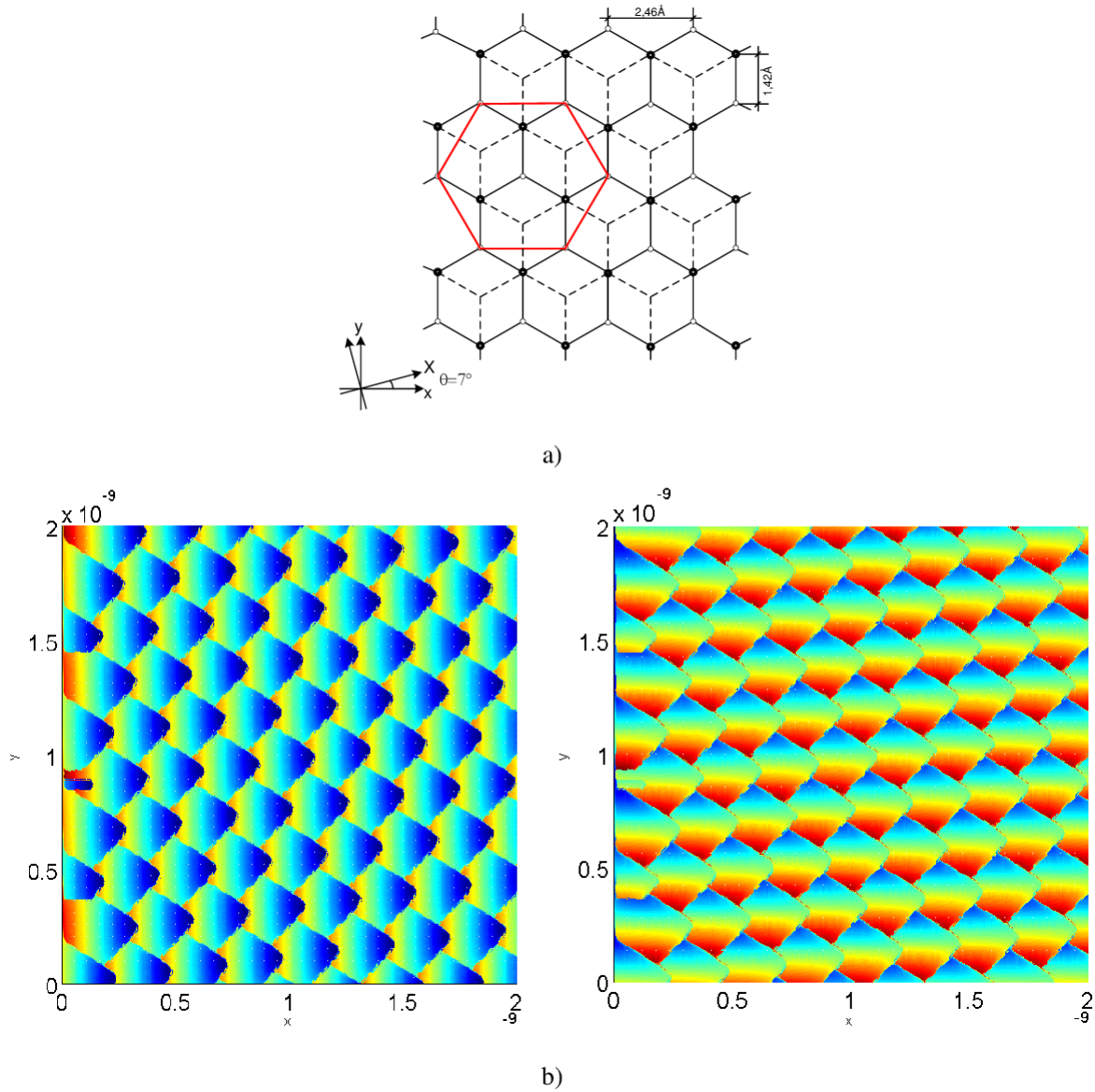


Figure 8 a) Position of the atoms in the HOPG crystal net; b) Elastic force in the tip:  $F_x$  in the left hand side and  $F_y$  in the right hand side.

Let us assumed that the inertial moment of the crank,  $J$ , is equal to  $m_c \cdot L^2/3$ . The dimensionless parameters, from the data above, are:  $\xi = 1/3 \cdot m_c/m = 0.412$  and  $\kappa = 1.5$ . The value of the modified gravity acceleration is:  $g' = g \cdot m/k_1 = 0.01778m$ .

The parameters that characterize the friction are:

- dimensionless accuracy parameter,  $\varepsilon' = 3.5121e7$
- dimensionless parameter in dynamic friction coefficient,  $\delta' = 3.5121$

The static friction coefficient,  $\mu_s$ , is calculated from a measure using a mass on the belt. A friction force of 1.6 N is obtained from a mass of 0.277 kg, which means a value of  $\mu_s$  equal to 0.59. The modified belt velocity



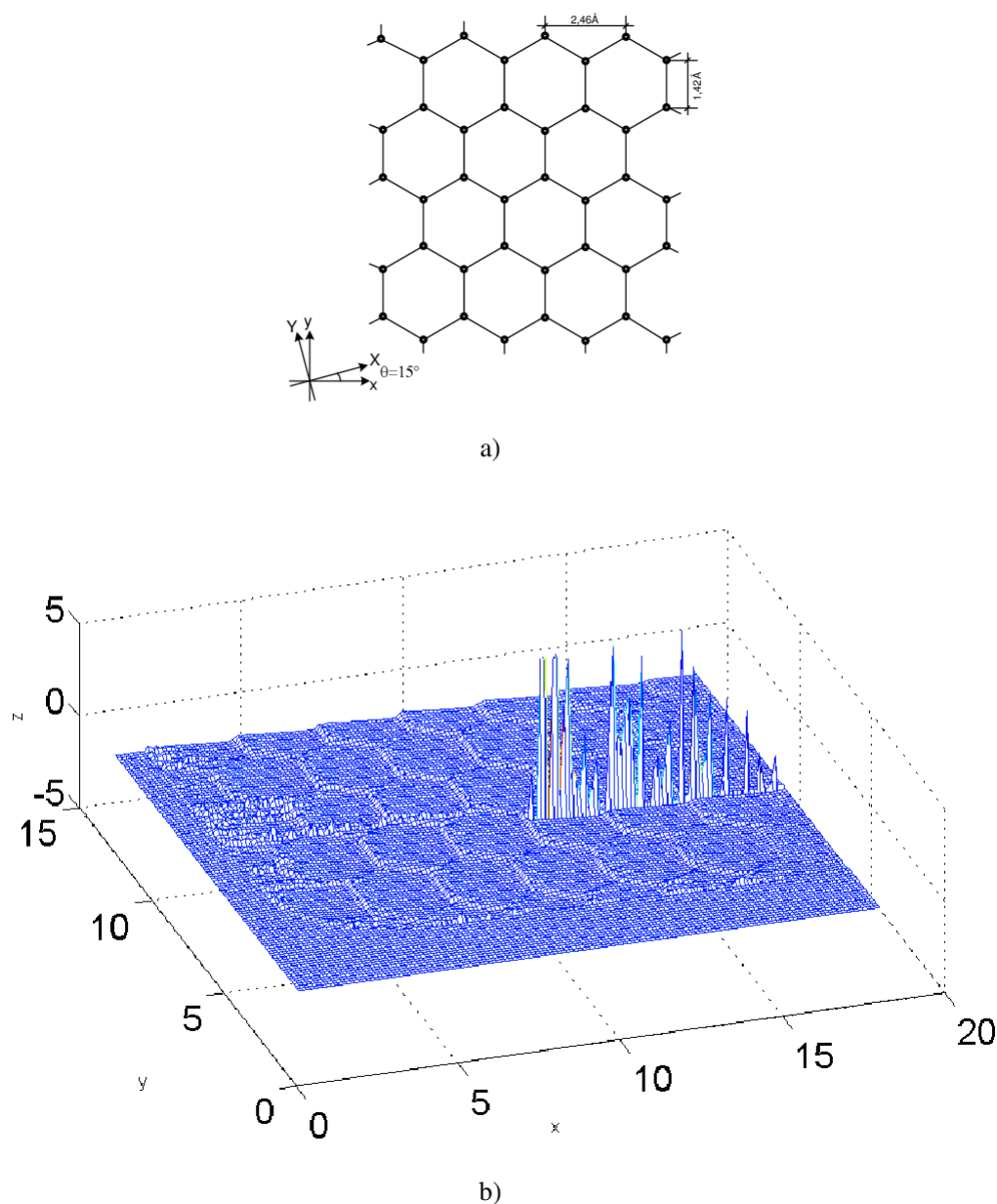


Figure 9 a) Position of the atoms in the HOPG crystal net; b) Elastic force in the tip,  $F_x$ .

used,  $v'_{dr}$ , is equal to  $-0.002788 \text{ m}$ .

Fig. 12 shows the phase plane for the belt velocity used for a time span from 100 to 1,000. Stick phase can be recognized as a horizontal line with ordinate  $V_1 = -0.002788 \text{ m}$ , Fig. 12. In addition, Fig. 13 shows the frequency spectrum of the signal  $X_1$  for a time span from 100 to 1,000.

A waveband arises centred on the value of  $0.143433 \text{ Hz}$ , a value that has no relation with belt velocity. Fig. 14 shows the Poincaré map using a period of  $1/0.143433$  for a time span from 0 to 3,200.

Fig. 14 shows the chaotic behaviour of the system. To quantify the chaos, an approximation to the maximum Lyapunov exponent is calculated from a time series of the solution by the software OpenTSTool [80], developed by Göttingen University. This approximate value is equal to  $0.0514$ , which suggests chaotic behavior of the

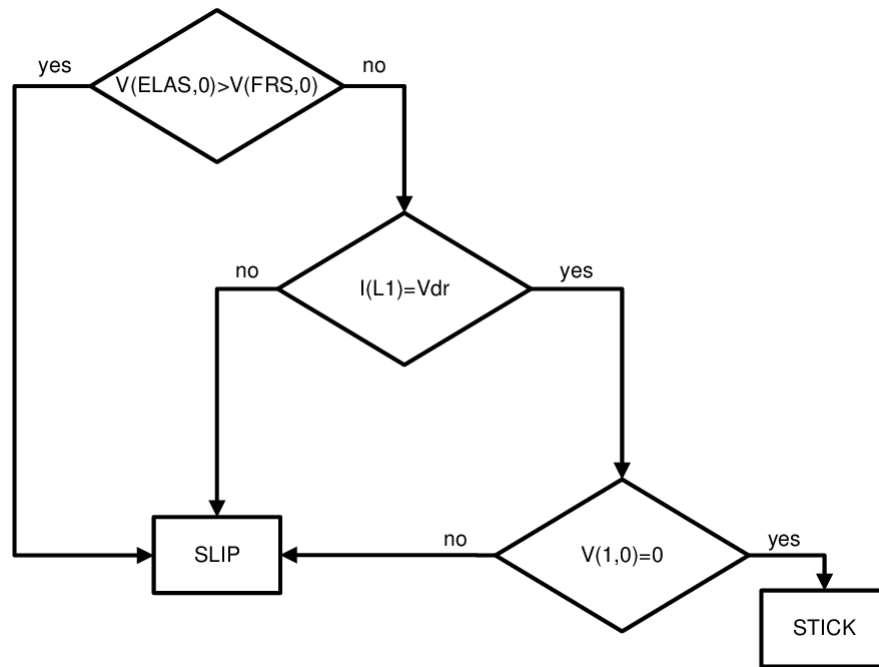


Figure 10 Decision algorithm used to control the switches.

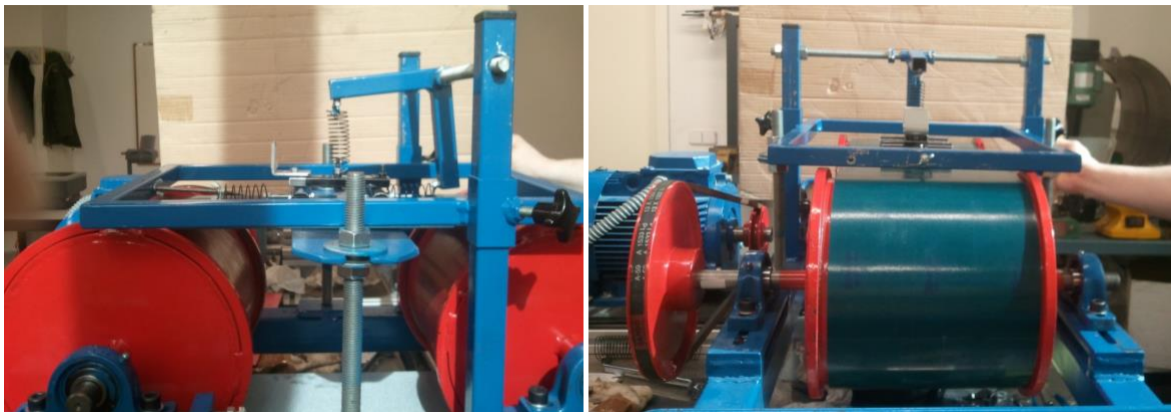


Figure 11 Mechanism.

solution.

## 7 Conclusions

A numerical model based on the network method has been designed to simulate several types of microscope and sample surfaces with different crystal nets. The results were successfully compared with those of different authors obtained with different methodologies. The software is flexible enough to implement the different values of the main parameters with no important changes, and allows different types of graph to be used. Thus, this software is able to manage different theoretical crystal nets, even with crystallographic defects, providing the corresponding theoretical elastic forces that can be compared with those obtained by microscope. Furthermore,

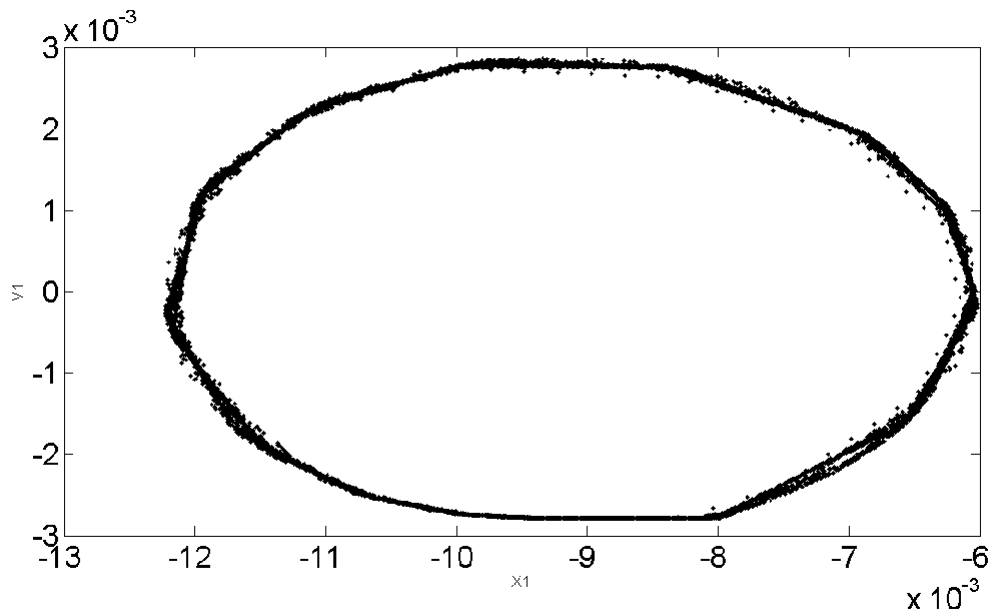


Figure 12 Phase plane:  $v'_{dr} = -0.002788m$ ;  $\xi = 0.412$ ;  $\kappa = 1.5$ .

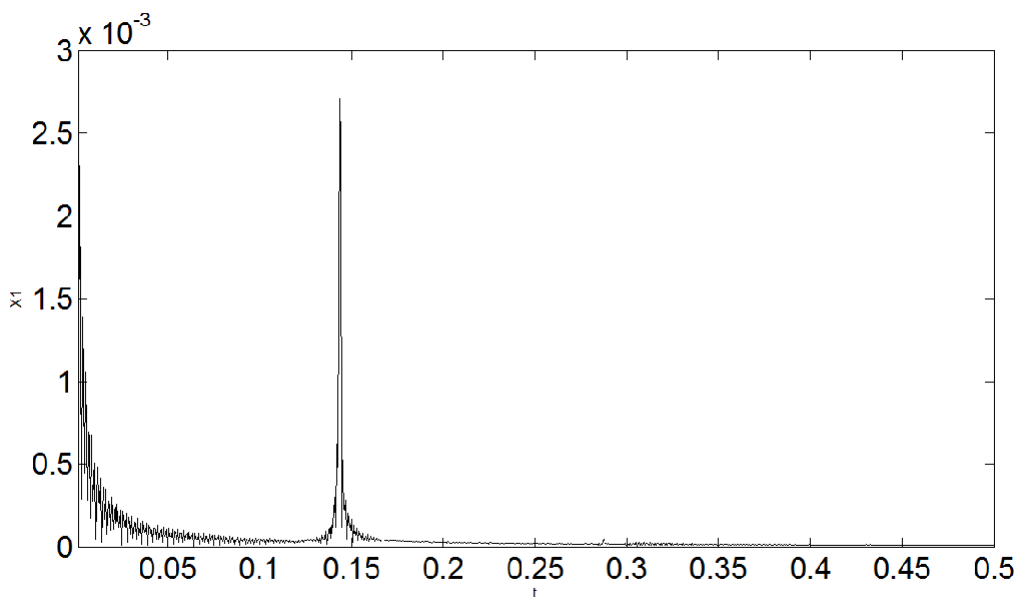


Figure 13 Frequency spectrum of  $X_1$ :  $v'_{dr} = -0.002788m$ ;  $\xi = 0.412$ ;  $\kappa = 1.5$ .

the short computational time necessary means that the software can be used to determine the values of the microscope parameters from experimental images of certain materials, whose data are not available. The calculated parameters allow other sample materials to be simulated. The final potential use of this software is to test the effect of microscope parameters on the quality of the image assisting to the use of the microscope.

Equations equivalent to those used by Awrejcewicz et al. have been developed, adapting them for the general

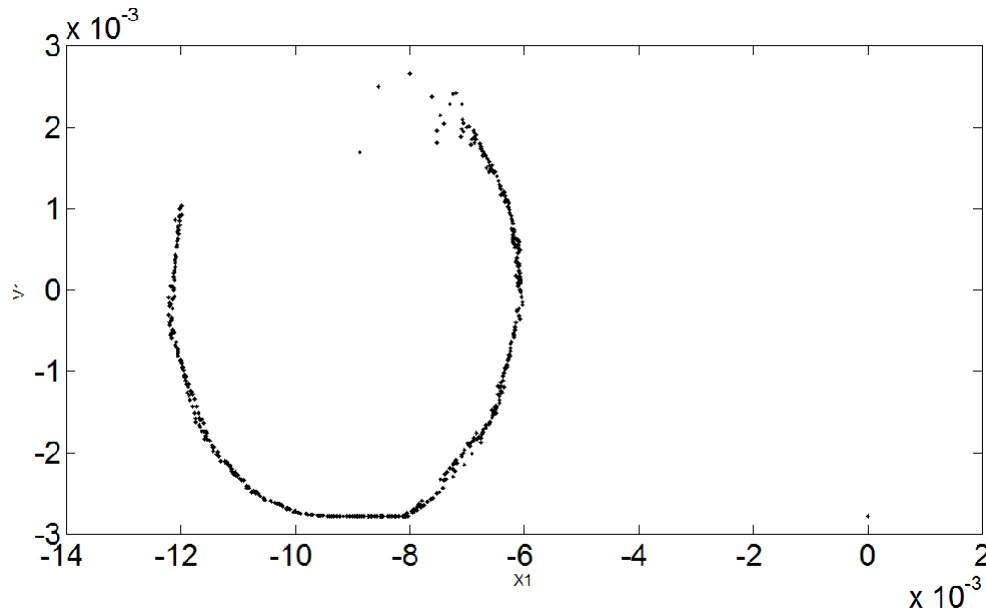


Figure 14 Poincaré map:  $\dot{v}_{dr} = -0.002788m$ ;  $\xi = 0.412$ ;  $\kappa = 1.5$ .

forms used in the analysis of different friction problems using the network method. Unlike, in the scheme proposed by these authors, we do not include horizontal and vertical damping, thus increasing the instability of the system and the difficulty of solving the problem. To save computational time, several parameterizations have been considered. As a result, the parameters in the left term of the first equation of the system in Eq. 10 are cancelled, speeding up the solution. The use of nondimensional time, useful in the solution to other friction problems, should be emphasised. Finally, it is necessary to evaluate the performance of the different tools to identify the chaotic behaviour. For this reason, the authors proved the current techniques, selecting the Poincaré map, frequency spectrum and maximum Lyapunov exponent because they better demonstrate such behaviour. Since the system jumps between two phases and it is not possible to use a Jacobian-based method, which would be more reliable, a direct method is used to calculate the maximum Lyapunov exponent. As all the references mention, this algorithm depends strongly on the embedding dimension and the time delay. Thus, the maximum Lyapunov exponent is difficult to specify, but in this work we are more interested in knowing the relative chaotic level than the absolute value. Another point that introduces uncertainty in the calculation of this exponent is the sample frequency necessary to obtain the data used in the algorithm.

## 8 Acknowledgments

We are grateful to Dr. J.A. Moreno, professor of the Mechanical Engineering Department in the Technical University of Cartagena, for some interesting and convenient tips about Network Simulation Method.

## References

- [1] González-Fernández, C.F. (2001), Heat transfer and the network simulation method. J. Horno (Ed.), Research Signpost, Trivandrum, India, p. 30.

- [2] Alarcón, M. (2001). Transporte de calor en sistemas con aletas. Coeficientes de rendimiento y red de transferencia. Física Aplicada. Universidad Politécnica de Cartagena.
- [3] Zueco, J. (2003). Solución de problemas inversos en conducción de calor mediante el método de simulación por redes. Física Aplicada. Universidad Politécnica de Cartagena
- [4] Castro, E. (2005). Simulación de ondas elásticas en vigas mediante el método de redes y detección de daño mediante la transformada wavelet. Física, Universidad de Jaén.
- [5] Soto, A. (2007). Simulación numérica de procesos de intrusión salina en acuíferos mediante el método de simulación por redes. Física Aplicada. Universidad Politécnica de Cartagena.
- [6] del Cerro, F. (2009). Desarrollo de un programa de conducción de calor, usando analogía eléctrica, mediante el lenguaje C y el módulo de cálculo Pspice. Aplicaciones lineales y no lineales en diferentes geometrías. Universidad de Murcia.
- [7] Luna, J.P. (2010). Caracterización, optimización y diseño de algunos tipos de aletas a través del concepto de admitancia térmica inversa relativa. Física Aplicada. Universidad Politécnica de Cartagena.
- [8] Alhama, F., López-Sánchez, J.F. et al. (1997). Heat conduction through a multilayered wall with variable boundary conditions. *Energy* 22(8): 797-803. doi [10.1016/S0360-5442\(97\)00003-0](https://doi.org/10.1016/S0360-5442(97)00003-0)
- [9] González-Fernández, C.F., Alhama, F. et al. (1998). Application of the network method to heat conduction processes with polynomial and potential-exponentially varying thermal properties. *Numerical Heat Transfer Part A–Applications* 33(5): 549-559. doi [10.1080/10407789808913954](https://doi.org/10.1080/10407789808913954)
- [10] Alarcón, M., Alhama, F. et al. (2002). Transient conduction in a fin-wall assembly with harmonic excitation -network thermal admittance. *Heat Transfer Engineering* 23(2): 31-43. doi [10.1080/01457630252800412](https://doi.org/10.1080/01457630252800412)
- [11] del Cerro, F., Gómez-Lopera, S.A. et al. (2008). A powerful and versatile educational software to simulate transient heat transfer processes in simple fins. *Computer Applications in Engineering Education* 16(1): 72-82. doi [10.1002/cae.20159](https://doi.org/10.1002/cae.20159)
- [12] Horno, J., García-Hernández, M.T. et al. (1993). Digital-simulation of electrochemical processes by the network approach. *Journal of Electroanalytical Chemistry* 352(1-2): 83-97. doi [10.1016/0022-0728\(93\)80256-H](https://doi.org/10.1016/0022-0728(93)80256-H)
- [13] Moya, A. (2011). Influence of DC electric current on the electrochemical impedance of ion-exchange membrane systems. *Electrochimica Acta* 56(8): 3015-3022. doi [10.1016/j.electacta.2010.12.103](https://doi.org/10.1016/j.electacta.2010.12.103)
- [14] Horno, J., González-Caballero, F. et al. (1990). The effect of previous convective flux on the nonstationary diffusion through membranes - network simulation. *Journal of Membrane Science* 48(1): 67-77. doi [10.1016/S0376-7388\(00\)80796-6](https://doi.org/10.1016/S0376-7388(00)80796-6)
- [15] Zueco, J., Alhama, F. et al. (2005). Inverse problem of estimating time-dependent heat transfer coefficient with the network simulation method. *Communications in Numerical Methods in Engineering* 21(1): 39-48. doi [10.1002/cnm.726](https://doi.org/10.1002/cnm.726)
- [16] Alhama, I., Soto, A. et al. (2011). FATSIM-A: An educational tool based on electrical analogy and the code PSpice to simulate fluid flow and solute transport processes. *Computer Applications in Engineering Education* 16: 72-84. doi [10.1016/j.icheatmasstransfer.2005.08.013](https://doi.org/10.1016/j.icheatmasstransfer.2005.08.013)
- [17] Alhama, I., Soto, A. et al. (2011). FATSIM-A: An educational tool based on electrical analogy and the code PSpice to simulate fluid flow and solute transport processes. *Computer Applications in Engineering Education* 16: 72-84.
- [18] Zueco, J. and Alhama, F. (2007). Simultaneous inverse determination of temperature-dependent thermophysical properties in fluids using the network simulation method. *International Journal of Heat and Mass Transfer* 50(15-16): 3234-3243. doi [10.1016/j.ijheatmasstransfer.2007.01.004](https://doi.org/10.1016/j.ijheatmasstransfer.2007.01.004)
- [19] Beg, O.A., Zueco, J. et al. (2009). Transient nonlinear optically-thick radiative-convective double-diffusive boundary layers in a darcian porous medium adjacent to an impulsively started surface: network simulation solutions. *Communications in Nonlinear Science and Numerical Simulation* 14(11): 3856-3866. doi [10.1016/j.cnsns.2009.01.033](https://doi.org/10.1016/j.cnsns.2009.01.033)
- [20] Soto, A., Alhama, F. et al. (2007). Density-Driven flow and solute transport problems. A 2D numerical model based on the network simulation method. *Computer Physics Communications* 177(9): 720-728. doi [10.1016/j.cpc.2007.06.008](https://doi.org/10.1016/j.cpc.2007.06.008)
- [21] Soto, A., Alhama, F. et al. (2007). An efficient model for solving density driven groundwater flow problems based on the network simulation method. *Journal of Hydrology* 339(1-2): 39-53. doi [j.jhydrol.2007.03.003](https://doi.org/10.1016/j.jhydrol.2007.03.003)
- [22] Alhama, I., Soto, A. et al. (2012). Simulation of flow and solute coupled 2D problems with velocity-dependent dispersion coefficient based on the network method. *Hydrological Processes* 26(24): 3725-3735. doi [10.1002/hyp.8457](https://doi.org/10.1002/hyp.8457)
- [23] Alcaraz, D., Alhama, F. et al. (2005). Influence of fiber distribution in the thermal continuity of composites with titanium and magnesium alloys matrix (in Spanish). *Revista Española de Metalurgia Extr.*: 293-303.
- [24] Moreno, J. A., Gómez, F.C. et al. (2007). Solution of temperature fields in hydrodynamics bearings by the numerical network method. *Tribology International* 40(1): 139-145. doi [10.1016/j.triboint.2006.03.008](https://doi.org/10.1016/j.triboint.2006.03.008)
- [25] Benavent, A., Castro, E. et al. (2010). Evaluation of low-cycle fatigue damage in RC exterior beam-column subassemblages by acoustic emission. *Construction and Building Materials* 24: 1830-1842. doi [10.1016/j.conbuildmat.2010.04.021](https://doi.org/10.1016/j.conbuildmat.2010.04.021)
- [26] Marín, F., Alhama, F. et al. (2012). Modelling of stick-slip behaviour with different hypotheses on friction forces. *International Journal of Engineering Science* 60: 13-24. doi [10.1016/j.ijengsci.2012.06.002](https://doi.org/10.1016/j.ijengsci.2012.06.002)
- [27] Morales, J.L., Moreno, J.A. et al. (2012). New additional conditions for the numerical uniqueness of the boussinesq and timpe solutions of elasticity problems. *International Journal of Computer Mathematics* 89(13-14): 1794-1807. doi [10.1080/00207160.2012.667088](https://doi.org/10.1080/00207160.2012.667088)

- [28] Gómez-Lopera, S., Alhama, F. et al. (2005). PRODASIM. Programa de diseño de aletas simples. N. 08/2005/544, Universidad Politécnica de Cartagena.
- [29] Alhama, F. and del Cerro, F. (2009). PROCCA. Programa de conducción de calor. N. 08/2005/544. Universidad Politécnica de Cartagena.
- [30] Alhama, I., Soto, A. et al. (2010). FATSIM-A. Fluid flow and solute transport simulator N. D. Mu-1093-2010). Universidad Politécnica de Cartagena.
- [31] Alhama, I., Soto, A. et al. (2010). FAHET. Flow and heat transport simulator. N. 08/2011/419. Cartagena, Universidad Politécnica de Cartagena.
- [32] Morales, J.L., Moreno, J.A. et al. (2010). EPSNET 10. Elasticity problems simulation network. N. 08/2011/418. Universidad Politécnica de Cartagena.
- [33] Sánchez, J.F., Moreno, J.A et al. (2013). OXIPSIS 12. N. Mu-751-2013. Universidad Politécnica de Cartagena.
- [34] Peusner, L. (1987). The principles of network thermodynamics: theory and biophysical applications. Entropy, Lincoln, USA.
- [35] Schwarz, U. D. and Hölscher, H. (2001). Atomic scale friction studies using scanning force microscopy. Modern Tribology Handbook. B. Bhushan (Ed.). CRC Press, Boca Ratón, Florida, USA: p. 593. doi [10.1201/9780849377877.ch18](https://doi.org/10.1201/9780849377877.ch18)
- [36] Hölscher, H., Schwarz, U.D. et al. (1996). Simulation of a scanned tip on a NaF(001) surface in friction force microscopy. Europhysics Letters 36(1): 19-24. doi [10.1209/epl/i1996-00181-4](https://doi.org/10.1209/epl/i1996-00181-4)
- [37] Hölscher, H., Schwarz, U.D. et al. (1998). Consequences of the stick - slip movement for the scanning force microscopy imaging of graphite. Physical Review B 57(4): 2477-2481. doi [10.1103/PhysRevB.57.2477](https://doi.org/10.1103/PhysRevB.57.2477)
- [38] Sasaki, N., Kobayashi, K. et al. (1996). Atomic - scale friction image of graphite in atomic-force microscopy. Physical Review B 54(3): 2138-2149. doi [10.1103/PhysRevB.54.2138](https://doi.org/10.1103/PhysRevB.54.2138)
- [39] Hölscher, H., Allers, W. et al. (2000). Interpretation of "true atomic resolution" images of graphite (0001) in noncontact atomic force microscopy. Physical Review B 62(11): 6967-6970. doi [10.1103/PhysRevB.62.6967](https://doi.org/10.1103/PhysRevB.62.6967)
- [40] Blau, P.J. (1986). Friction Science and Technology. Marcel Dekker, New York.
- [41] Dowson, D. (1998). History of Tribology. Professional Engineering Publishers, London.
- [42] Perry, S.S. (2001). Progress in the pursuit in the fundamentals of tribology. Tribology Letters 10(1-2), 1-4. doi [10.1023/A:1009034614549](https://doi.org/10.1023/A:1009034614549)
- [43] Blau, P.J. (2001). The significance and use of the friction coefficient. Tribology International 34, 585-591. doi [S0301-679X\(01\)00050-0](https://doi.org/10.1016/S0301-679X(01)00050-0)
- [44] Müser, M.H. (2006). Theory and simulation of friction and lubrication. Lecture Notes Physics 704, 65. doi [10.1007/3-540-35284-84](https://doi.org/10.1007/3-540-35284-84)
- [45] Hess, D.P., Soom, A. (1990). Friction at a lubricated line contact operating at oscillating sliding velocities. Journal of Tribology Transactions ASME 112(1), 147-152. doi [10.1115/1.2920220](https://doi.org/10.1115/1.2920220)
- [46] Armstrong-Hélouvy, B. (1991). Control Mach. Frict. Kluwer Academic Press, Hingham.
- [47] Courtney-Pratt, J.S., Eisner, E. (1956). The effect of a tangential force on the contact of metallic bodies. Proceedings of the Royal Society A 238, 529-550. doi [10.1098/rspa.1957.0016](https://doi.org/10.1098/rspa.1957.0016)
- [48] Liang, J.W., Feeny, B.F. (1998). A comparison between direct and indirect friction measurements in a forced oscillator. Journal of Applied Mechanics Transactions ASME 65(3), 783-786. doi [10.1115/1.2789129](https://doi.org/10.1115/1.2789129)
- [49] Powell, J., Wiercigroch, M. (1992). Influence of non-reversible Coulomb characteristics on the response of a harmonically excited linear oscillator. Machinery Vibration. 1(2), 94-104.
- [50] Johannes, V.I., Green, M.A., Brockley, C.A. (1973). Role of rate of application of tangential force in determining static friction coefficient. Wear 24(3), 381-385. doi [10.1016/0043-1648\(73\)90166-X](https://doi.org/10.1016/0043-1648(73)90166-X)
- [51] Rabinowicz, E.J. (1951). The nature of the static and kinetic coefficients of friction. Journal of Applied Physics 22(11), 1373-1379. doi [10.1063/1.1699869](https://doi.org/10.1063/1.1699869)
- [52] Stribeck, R. (1902). Fundamental characteristics of the friction bearing and the roller bearing. Zeitschrift des Vereines Deutscher Ingenieure 46(46), 1341-1348.
- [53] Wojewoda, J., Stefanski, A., Wiercigroch, M., Kapitaniak, T. (2009). Estimation of Lyapunov exponents for a system with sensitive friction model. Archives in Applied Mechanics 79(6-7), 667-677. doi [10.1007/s00419-008-0291-9](https://doi.org/10.1007/s00419-008-0291-9)
- [54] Coulomb, C.A. (1785). Théorie des machines simples. Mémoire de Mathématiques et de Physique de l'Académie royale des Sciences 10, 161-182.
- [55] Stefanski, A., Wojewoda, J., Wiercigroch, M., Kapitaniak, T. (2003). Chaos caused by non-reversible dry friction. Chaos Solitons Fractals 16(5), 661-664. doi [10.1016/S0960-0779\(02\)00451-4](https://doi.org/10.1016/S0960-0779(02)00451-4)
- [56] Awrejcewicz, J., Olejnik, P. (2005). Analysis of dynamic system with various friction laws. Applied Mechanics Review 58(6), 389-411. doi [10.1115/1.2048687](https://doi.org/10.1115/1.2048687)
- [57] Fu, W.P., Fang, Z.D., Zhao, Z.G. (2001). Periodic solutions and harmonic analysis of an anti-lock brake system with piecewise nonlinearity. Journal of Sound and Vibration 246(3), 543-550. doi [10.1006/jsvi.2001.3599](https://doi.org/10.1006/jsvi.2001.3599)
- [58] Choi, H.S., Lou, J.Y.K. (1991). Nonlinear behaviour and chaotic motions of an sdof system with piecewise non-linear stiffness. International Journal of Non-linear Mechanics 26(5), 461-473. doi [10.1016/0020-7462\(91\)90002-b](https://doi.org/10.1016/0020-7462(91)90002-b)
- [59] Fling, R.T., Fenton, R.E. (1981). A describing-function approach to antiskid design. IEEE Transactions on Vehicle



- Technology 30(3), 134-144. doi [10.1109/T-VT.1981.23895](https://doi.org/10.1109/T-VT.1981.23895)
- [60] Perko, L. (1991). *Differential Equations and Dynamical Systems*. Springer, New York. doi [10.1007/978-1-4684-0392-3](https://doi.org/10.1007/978-1-4684-0392-3)
- [61] Yeh, E.C., Day, G.C. (1992). Parametric study of antiskid brake systems using Poincaré map concept. *International Journal of Vehicle Des.* 13,210-232.
- [62] Girling Auto website <http://www.girlingauto.com>
- [63] Awrejcewicz, J., Olejnik, P. (2003). Numerical and experimental investigations of simple non-linear system modelling a Girling duo-servo brake mechanism. In: *Proceedings of DETC'03 ASME, Chicago*.
- [64] Awrejcewicz, J., Olejnik, P. (2007). Occurrence of stick-slip phenomenon. *Journal of Theoretical and Applied Mechanics* 45(1), 33-40.
- [65] Awrejcewicz, J., Olejnik, P. (2003). Improvement of the Lyapunov exponents computations by extension of time series. In: *Proceedings of the 11th World Congress in Mechanism and Machine Science, Tianjin, China*
- [66] Marín, F., Alhama, F., Moreno, J.A. (2014). Modelling of nanoscale friction using network simulation method. *Computers, Materials and Continua* 43(1), 1-19. doi [10.3970/cmc.2014.043.001](https://doi.org/10.3970/cmc.2014.043.001)
- [67] Marín, F., Alhama, F., Meroño, P.A., F., Moreno, J.A. (2016). Modelling of stick-slip behaviour in a Girling Brake using network simulation method. *Nonlinear Dynamics* 84(1), 153-162. doi [10.1007/s11071-015-2312-x](https://doi.org/10.1007/s11071-015-2312-x)
- [68] Microsim Corporation Fairbanks (1994) PSpice 6.0, Irvine, California.
- [69] Nagel, L.W. (1975). SPICE2: A Computer Program to Simulate Semiconductor Circuits. University of California, Berkeley.
- [70] Kreith, F. (2000). *The CRC Handbook of Thermal Engineering*. CRC Press, London.
- [71] Mills, A.F. (1998). *Heat Transfer*. Prentice Hall, Concord.
- [72] González-Fernández, C.F., Alhama, F., López-Sánchez, J.F. (1998). Application of the network method to heat conduction processes with polynomial and potential-exponentially varying thermal properties. *Numerical Heat Transfer Part A Applications* 33(5), 549-559. doi [10.1080/10407789808913954](https://doi.org/10.1080/10407789808913954)
- [73] Horno, J., González-Fernández, C.F., Hayas, A. (1995). The Network Method for solutions of oscillating reaction-diffusion systems. *Journal of Computational Physics* 118(2), 310-319. doi [10.1006/jcph.1995.1101](https://doi.org/10.1006/jcph.1995.1101)
- [74] Soto, A., Alhama, F., González-Fernández, C.F. (2007). An efficient model for solving density driven groundwater flow problems based on the network simulation method. *Journal of Hydrology* 339(1-2), 39-53. doi [10.1016/j.jhydrol.2007.03.003](https://doi.org/10.1016/j.jhydrol.2007.03.003)
- [75] Zueco, J., Alhama, F. (2006). Inverse determination of heat generation sources in two-dimensional homogeneous solids: application to orthotropic medium. *International Communications in Heat Mass Transfer* 33(1), 49-55. doi [10.1016/j.icheatmasstransfer.2005.08.013](https://doi.org/10.1016/j.icheatmasstransfer.2005.08.013)
- [76] Van de Vrande, B.L., Van Campen, D.H., De Kraker, A. (1999). An approximate analysis of dry-friction-induced stick-slip vibrations by a smoothing procedure. *Nonlinear Dynamics* 19, 157-169. doi [10.1023/A:1008306327781](https://doi.org/10.1023/A:1008306327781)
- [77] Elmer, F.J. (1997). Nonlinear dynamics of dry friction. *Journal of Physics A Math. Gen.* 30(17), 6057-6063. doi [10.1088/0305-4470/30/17/015](https://doi.org/10.1088/0305-4470/30/17/015)
- [78] Vladimirescu, A. (1994). *The SPICE Book*. Wiley, New York.
- [79] Kielkowski, R. (1994). *Inside SPICE*. McGraw Hill, New York.
- [80] Merkwirth, C., Parltitz, U., Wedekind, I., Engster, D., Lauterborn, W. (2009). *OpenTSTOOL User Manual Version 1.2* (2/2009). Drittes Physikalisches Institut. Universität Göttingen.